UV-Induced Reaction Kinetics of Dilinoleoylphosphatidylethanolamine Monolayers

Tapani Viitala and Jouko Peltonen
Department of Physical Chemistry, Åbo Akademi University, FIN-20500 Turku, Finland

ABSTRACT The UV-induced reactivity of dilinoleoylphosphatidylethanolamine (DLiPE) Langmuir and Langmuir-Blodgett films has been studied by in situ measurements of the changes in the mean molecular area, UV-vis and Fourier transform infrared spectroscopy, and atomic force microscopy (AFM). Optimum orientation and packing density of the DLiPE molecules in the monolayer were achieved by adding uranyl acetate to the subphase. A first-order reaction kinetic model was successfully fitted to the experimental reaction kinetics data obtained at a surface pressure of 30 mN/m. Topographical studies of LB films by AFM were performed on bilayer structures as a function of subphase composition and UV irradiation time. The orientational effect of the uranyl ions on the monolayer molecules was observed as an enhanced homogeneity of the freshly prepared monomeric LB films. However, the long-term stability of these films proved to be bad; clear reorganization and loss of a true monolayer structure were evidenced by the AFM images. This instability was inhibited for the UV-irradiated films, indicating that the UV irradiation gave rise to a cross-linked structure.

INTRODUCTION

Langmuir-Blodgett (LB) films are characterized by a high degree of molecular orientation in ultrathin structures, which may offer unique applications, e.g., in the field of biocompatible materials (Roberts, 1990). The required stability for potential applications may be provided by using different kinds of polymeric materials. The use of preformed polymers (Brinkhuis and Schouten, 1991; Yang et al., 1994; Wang et al., 1995) or the polymerization of reactive amphiphiles as a Langmuir monolayer (Dubault et al., 1975; Ringsdorf and Schupp, 1982; Bodalia and Duran, 1993; Peltonen et al., 1994; Tillmann et al., 1994) or as a multilayer deposited on a solid substrate (Tieke et al., 1979; Warta and Sixl, 1988; Mino et al., 1991; Peltonen et al., 1993; Miyashita and Ito, 1995) are promising methods for improving the mechanical, chemical, and thermal properties of organic thin films. Because monolayers of preformed polymers are occasionally difficult to process because of their high viscosity and inhomogeneous distribution at the air/water interface, the polymerization of monomeric monolayers before or after deposition has gained considerable interest. Diacetylenes, dienes, and vinyl derivatives are the most commonly studied molecules in this class (Meller et al., 1989; Arslanov, 1992).

Ultraviolet light is most commonly used as the initiator of polymerization of monomeric Langmuir and Langmuir-Blodgett films, even though higher energy radiation (Cemel et al., 1972; Ogawa, 1989) and catalysts in the subphase (Bodalia and Duran, 1993) have been used. If polymerization is performed at the air/water interface, it can in many cases be followed in situ by measuring the changes in the mean molecular area and barrier speed (Ringsdorf and Schupp, 1982; Arslanov, 1992; Bodalia and Duran, 1993; Peltonen et al., 1994). In a special case, however, topochemical polymerization takes place, which means that the crystal structure remains unchanged and no area contraction occurs during the reaction (Wegner, 1969). The polymerization reaction can also be followed ex situ by various complementary techniques such as surface viscosity (Dubault et al., 1975; Rolandi et al., 1995), atomic force microscopy (Peltonen et al., 1993; Tillmann et al., 1994; Rolandi et al., 1995), fluorescence microscopy (Warta and Sixl, 1988; Meller et al., 1989; Rolandi et al., 1995), UV-vis (Tieke et al., 1979; Laschewsky et al., 1988; Mino et al., 1991; Viitala et al., 1997), and IR spectroscopy (Letts et al., 1976; Lindén et al., 1995).

The theoretical treatment of a reaction performed on a monolayer is not as straightforward as it seems to be, and models for three-dimensional reaction kinetics cannot be directly applied because of the peculiar features of a two-dimensional system (Raudino, 1994; Rolandi et al., 1995). Successful attempts at modeling the reaction kinetics of a floating monolayer have been made by a few research groups (Bodalia and Duran, 1993; Rolandi et al., 1995; Viitala et al., 1997). The results have been in very good correlation with the experimental data for the studied systems.

We have studied the UV-induced reactivity of several unsaturated fatty acids with one or two nonconjugated double bonds in the middle of the hydrocarbon chains (Peltonen et al., 1992, 1993, 1994; Lindén et al., 1995). The fastest reaction rate was observed for linoleic acid (LA) on subphases containing trivalent metal ions (Peltonen et al., 1994; Lindén et al., 1995). A very simple first-order model for the reaction kinetics giving a reasonable fit to the experimental data was presented. This model, however, was based on quite strong simplifying assumptions and was later revised

Received for publication 16 March 1998 and in final form 18 December 1998.

Address reprint requests to Dr. Tapani Viitala, Department of Physical Chemistry, Åbo Akademi University, Porthansgatan 3-5, FIN-20500 Turku, Finland. Tel.: +358-2-2154252; Fax: +358-2-2154706; E-mail: tviitala@abo.fi.

0006-3495/99/05/2803/11 $2.00

by taking into account the time-dependent change in the mean molecular area during UV irradiation (Viitala et al., 1997).

The aim of this paper is to study the monolayer behavior and reactivity of an LA lipid derivative, dilinoleoylphosphatidylethanolamine (DLiPE), on different subphases. The validity of the previously presented reaction kinetic model for LA is further confirmed by applying the model to the DLiPE reaction kinetics data. Future interest lies in the study of reactive biofunctional films, i.e., mixed films of DLiPE and its synthesized derivative incorporating a linker unit, capable of immobilizing antibodies.

MATERIALS AND METHODS

1,2-Dilinoleoyl-s,n-glycero-3-phosphatidylethanolamine (DLiPE) (> 99% purity) was obtained from Avanti Polar Lipids (Alabaster, AL). Chloroform of high-performance liquid chromatography grade, used as a spreading solvent (1 mg/ml) for DLiPE, was obtained from Sigma (Deisenhofen, Germany). NaCl, uranyl acetate (UAc), Tris(hydroxymethyl)aminomethane (Tris), all of PA grade, and Titrisols (NaOH and HCl) were obtained from Merck (Darmstadt, Germany). Stearic acid (SA) (99% purity), $TbCl_3$ (better than 98% purity), and *n*-hexane (<99.5%) used as the spreading solvent (1 mg/ml) for SA, were all obtained from Fluka (Buchs, Switzerland). The chemicals were used as received. The solution of DLiPE was protected against light and stored in a freezer under argon until spreading. The water used to prepare the subphase was purified with a Millipore Milli-Q filtering system (Bedford, MA).

Computerized barostats KSV2000 and KSV5000 (KSV Instruments, Helsinki, Finland) were used for L and LB film preparation. The surface pressure was measured with the Wilhelmy plate technique. The compression of the monolayers was started 10 min after spreading. After reaching the target pressure, the monolayer was allowed to equilibrate for 10–15 min before deposition or UV irradiation. Langmuir films of DLiPE were prepared on four different subphases, which are referred to in the text by the abbreviations in parentheses: pure ion-exchanged water, pH 5.6 (IEW); 10^{-3} M uranyl acetate in ion-exchanged water, pH 4.7 (IEW/UAc); 10^{-3} M Tris + 0.1 M NaCl in ion-exchanged water, pH 7.2 (Tris/NaCl); and 10^{-3} M Tris + 0.1 M NaCl + 10^{-5} M UAc in ion-exchanged water, pH 7.2 (Tris/NaCl/UAc). All Langmuir film experiments were performed at a constant temperature of 20 ± 0.5°C.

The DLiPE LB films were deposited vertically at a surface pressure of 30 mN/m with a dipping speed of 5 mm/min on quartz/Tb stearate slides for UV-vis analysis and on mica/Tb stearate substrates for AFM measurements. The quartz slides were cleaned by first immersing them in a chromic acid solution overnight, then neutralizing them in a 0.01 M NaOH solution for ~24 h, and finally rinsing with ethanol and ion-exchanged water. The mica plates were freshly cleaved before deposition. The Tb stearate layer on quartz and mica substrates was deposited from a 10^{-4} M $TbCl_3$ subphase with pH 5 at a surface pressure of 30 mN/m with a dipping speed of 10 mm/min. Monomeric and UV-irradiated LB films were analyzed by a computer-controlled Schimadzu 240 UV-vis spectrometer (Schimadzu Co., Kyoto, Japan) operated at room temperature (~21°C). A 2 nm slit was used. As a reference, a spectrum for the cleaned quartz slide was measured before the deposition, which was then subtracted from the spectra obtained for the LB films. The solution spectra were measured with a 10-mm optical path quartz cuvette. A DLiPE multilayer structure was further deposited horizontally from a IEW/UAc subphase onto a ZnSe ATR crystal (dimensions: 50 × 12 × 3 mm^3) for analysis with a Bruker FRA 106 Fourier transform infrared (FTIR) spectrometer (Bruker, Karlsruhe, Germany).

A Nanoscope III (Digital Instruments, Santa Barbara, CA) AFM in tapping mode was used to image the LB samples. The imaging was performed in air, using a J-scanner (150 × 150 μm^2 scan range) with etched silicon cantilevers supplied by the manufacturer (Nanoprobes). The following parameters were characteristic of the used cantilevers: force constant between 20 and 100 N/m, resonance frequency of 270–300 kHz, nominal tip radius of curvature of 5–10 nm, cantilever length 129 μm, and pyramidal tip shape. The free amplitude of the cantilever (off contact) was chosen to be 100 nm, and imaging was carried out at moderate or light tapping conditions (0.50–0.85 set-point–free amplitude ratio).

The UV-induced reaction of the monolayers was carried out at a constant predetermined surface pressure. The surface pressure was kept constant during the reaction by adjusting and recording the monolayer area. The irradiation was performed in air by a 30-W low-pressure mercury lamp placed 0.2 m above the monolayer. The lamp had its maximum emission at 254 nm; other emission lines at longer wavelengths were negligible in intensity. The reactivity of monomeric LB films was also followed by measuring the UV-vis spectra for the LB films after different irradiation times. The monomeric LB films were placed 0.2 m from the lamp and irradiated in air, after which the UV-vis spectra were measured. The response of the monolayer to UV-irradiation depended only slightly on whether the curing was carried out under safety gas (N_2 or Ar) or air. The tightly packed film seemed to make the cross-linking reaction insensitive to quenching by oxygen radicals, which obviously exist in marked amounts in close proximity to the monolayer.

RESULTS AND DISCUSSION

Compression isotherms

Fig. 1 shows the molecular structure and the monolayer behavior of DLiPE on four different subphases. The introduction of *cis* double bonds in the alkyl chains is known to increase the mean molecular area as compared with saturated linear molecules. This makes it difficult to obtain a monolayer with closely packed DLiPE molecules at the air/water interface, not only because of sterical hindrance, but also because of the rather strong attractive interaction of the double bonds with the liquid subphase. Consequently, the DLiPE monolayer on an IEW subphase remained in a liquid-expanded (LE) state throughout the compression (Fig. 1 *b*), which is consistent with earlier reports concerning, e.g., dioleoyl-PE (DOPE) (Chapman et al., 1966) and dioleoyl-PC (DOPC) (phosphocholine) (Tancrede et al., 1981). The almost identical extrapolated mean molecular area of ~80 $Å^2$/molecule obtained for DLiPE, DOPE, and DOPC shows that the packing of the molecules at high surface pressure is controlled by the *cis*-unsaturated acyl chains and is almost independent of the degree of unsaturation. This agrees with an earlier report in which practically identical isotherms were observed for oleic and linoleic acids (Peltonen and Rosenholm, 1989). Special attention was paid to obtaining a more condensed monolayer by a proper choice of the subphase composition. A condensed monolayer has in many cases been found to be a prerequisite for an enhanced reactivity of a monomeric monolayer (Tieke et al., 1977; Ringsdorf and Schupp, 1982; Viitala et al., 1997).

Fig. 1 *b* shows the isotherms of DLiPE on IEW (pH 5.6) and IEW/UAc (pH 4.7) subphases. The different pH values are due to lowering of pH when the UAc is dissolved in IEW. This pH was not adjusted to 5.6 because we wanted to avoid the introduction of any additional ions into the system. The extrapolated mean molecular area of DLiPE on an IEW and IEW/UAc subphase was 82 and 66 $Å^2$, respec-

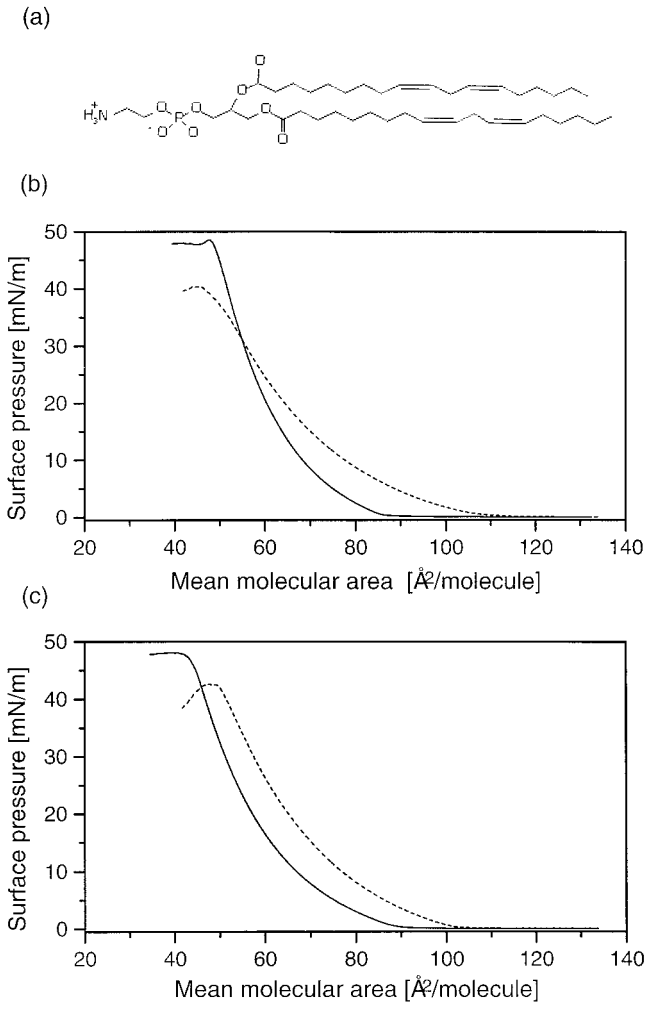

FIGURE 1 (*a*) Molecular structure of DLiPE. Compression isotherms of DLiPE on four different subphases. (*b*) IEW, pH 5.6 (– – –), and IEW/UAc, pH 4.7 (——). (*c*) Tris/NaCl, pH 7.2 (– – –), and Tris/NaCl/UAc, pH 7.2 (——).

tively. The most condensed state could not be achieved until a sufficient amount of UAc (i.e., 10^{-3} M) was introduced into the subphase. The condensing effect of UAc ions could also be seen as a decreasing A_i (onset of the initial pressure increase) value, decreased compressibility, and a higher fracture pressure. Thus the introduction of a sufficient amount of UAc into the subphase led to a more condensed, more stable, and elastic monolayer as compared to a monolayer formed on an IEW subphase. The monolayer had reached a state that we have referred to earlier, in the case of LA on a Tb-subphase, as the solid-expanded (SE) state (Peltonen et al., 1994; Lindén et al., 1995; Viitala et al., 1997).

Fig. 1 *c* shows the isotherms of DLiPE on Tris/NaCl and Tris/NaCl/UAc subphases, both measured at pH 7.2. The respective extrapolated mean molecular areas are now 76 and 64 Å^2. The more condensed monolayer obtained on a Tris/NaCl buffer subphase than on an IEW subphase is probably due to the interaction of Na^+ and Cl^- ions with the negative phosphate and positive amine groups in the polar headgroup, consequently reducing the repulsive interaction between the headgroups. This assumption is also justified by the fact that the zwitterionic phosphoethanolamine polar headgroup most likely has a horizontal orientation, which implies that the charge centers in the headgroup are readily accessible to the subphase ions (Tocanne and Teissié, 1990; Gorwyn and Barnes, 1990). The introduction of a minor amount of UAc to the Tris/NaCl buffer subphase induced a marked condensation of the monolayer similar to that observed for the IEW subphase. That the much larger amount of UAc needed to be introduced in the IEW subphase than in the Tris/NaCl subphase is probably due to the different pH value and ionic strength of the subphases, which affects both the solution chemistry of the UAc ions and the dissociation degree of the monolayer molecules (screening effect). UAc forms many different kinds of hydrolyzed species as a function of pH (Toth and Begun, 1981; Gorwyn and Barnes, 1990; Peñacorada et al., 1995). The different species were presented by Gorwyn and Barnes (1990), who studied the influence of UAc on phospholipid monolayers, using the following equilibria:

$$UO_2^{2+} \leftrightarrow (UO_2)(OH)_2^{2+} \leftrightarrow (UO_2)_3(OH)_5^{+} \leftrightarrow UO_2(OH)^{+}$$

There is a considerable overlap of the distribution curves in the pH range 3–7, where all of the above-listed species are present to some extent. Gorwyn and Barnes (1990) suggested that the condensation of the phospholipid monolayers induced by UAc is due to the adsorption of the ions to the monolayer by electrostatic attraction between the positive uranyl ions and the negatively charged phosphate groups. They concluded that at pH 5 the main ion adsorbing to the monolayer is $(UO_2)_2(OH)_2^{2+}$ with some UO_2^{2+}, and at pH 7 it is almost entirely $(UO_2)_2(OH)_2^{2+}$.

Applying this information to our results leads to the conclusion that the uranyl species responsible for the condensation of DLiPE at pH 4.7 are mainly $(UO_2)_2(OH)_2^{2+}$ with some UO_2^{2+}, and at pH 7.2 it is entirely $(UO_2)_2(OH)_2^{2+}$. Even if the condensing effect of the counterions used is obvious for DLiPE monolayers, the close packing of the monolayer molecules and the final extrapolated mean molecular area are probably determined by the unsaturated alkyl chains, because the mean molecular area is approximately the same for DLiPE on both UAc-containing subphases, even though the subphase conditions are completely different.

UV-vis spectroscopy

Fig. 2 shows the UV-vis spectra of DLiPE measured in hexane, ethanol, and chloroform and as an LB multilayer structure deposited from a Tris/NaCl/UAc subphase. Each spectrum shows only one distinct absorbance band located at 198, 206, 242, and 235 nm for the hexane, ethanol, and chloroform solutions and the LB film, respectively. These absorbance bands are attributed to the double bonds located in the middle of the hydrocarbon chains. The spectrum for

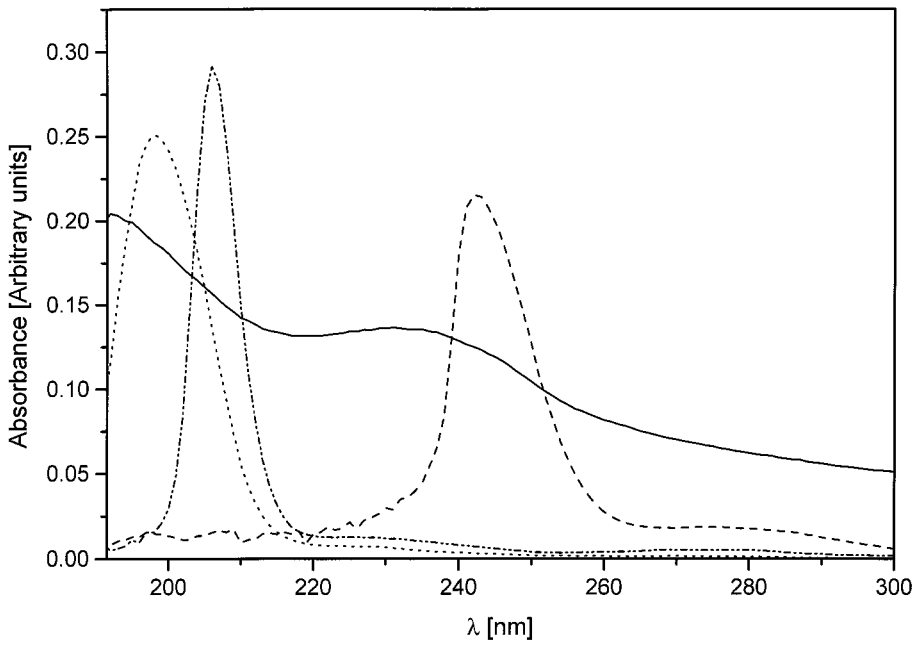

FIGURE 2 UV-vis spectra of DLiPE in hexane (- - -), ethanol (– ·· –), chloroform (– – –), and as an LB film deposited at 30 mN/m from a Tris/NaCl/UAc (pH 7.2) subphase (——).

the LB film deposited from an IEW/UAc subphase had the same form as that shown for the LB film in Fig. 2. The differences in the absorbance bands measured in solution and in an LB film are attributed to different molecular environments. The absorption bands measured in hexane and ethanol correspond to the well-known energy of an isolated double bond. The difference between these two solvents is due to a solvent effect that typically causes a redshift with increasing polarity of the solvent (Williams and Fleming, 1966). Chloroform acts quite differently from the other solvents. The pronounced redshift possibly reflects the formation of a charge transfer complex between the solvent and the surfactant, where the solvent carrying the very electronegative chlorine may act as an acceptor (Tamres and Yarwood, 1973). The absorbance band of the LB film is devoid of vibrational structure and is clearly broader than the absorbance bands measured in solution. This is a consequence of stronger intermolecular interactions in the densely packed LB film structure, which induce the formation of a variety of coexisting aggregated structures (Turro, 1978) as compared with the molecules in solution. However, the aggregates being formed by identical molecules cannot be called charge transfer complexes, but rather reflect to a delocalized p-electron system of interacting molecules. This consequently enables the initiation of a cross-linking reaction of a DLiPE monolayer by UV light. This situation seems comparable to a polymerizable fatty acid molecule with three conjugated double bonds in the hydrocarbon chain, giving a characteristic UV absorption band at 242 nm (Fukuda et al., 1988).

Reactivity measurements

The UV-induced reactivity of the UAc-DLiPE monolayers was followed in situ by recording the changes in the mean molecular area and barrier speed necessary to maintain the predetermined surface pressure. Fig. 3 shows the result for a typical measurement for a DLiPE monolayer on a Tris/NaCl/UAc subphase at a surface pressure of 30 mN/m. Exactly the same features were found for a monolayer UV-irradiated on a IEW/UAc subphase. The results of these measurements were quite similar to those obtained for LA on terbium or aluminum subphases (Peltonen et al., 1994; Lindén et al., 1995), i.e., the barrier speed reached a maximum after the monolayer had been UV-irradiated for 2.5 min, after which it began to decrease exponentially and finally reached a constant value. The reaction was completed within 15–20 min, whereas in the absence of UAc the reaction of the more expanded monolayer did not even reach a 50% yield after 120 min of UV irradiation. The high sensitivity of the reactivity to monolayer density means that cleavage of the hydrocarbon chains of individual lipids by UV light is ruled out. The compression corresponds to a considerable decrease in the mean molecular area. For the theoretical treatment of the reaction kinetics data, the measured mean molecular area was corrected (Fig. 3, *dashed line*) by assuming that the almost constant barrier movement measured after 20–40 min was due to the irradiation-induced instability of the monolayer (Viitala et al., 1997).

The UV irradiation of the monolayers was also performed at surface pressures of 10 and 20 mN/m. At these conditions the contraction of the monolayer was preceded by an expansion of the monolayer. The expansion was larger at lower surface pressures. This expansion is most obviously connected to the low density of the lipids, which increases the probability of free oxygen radical addition to the reaction centers. The consequent oxidation or even degradation of the monomers may take place, showing how sensitive the system is to the surface pressure; the expansion was not observed for monolayers compressed to a high pressure,

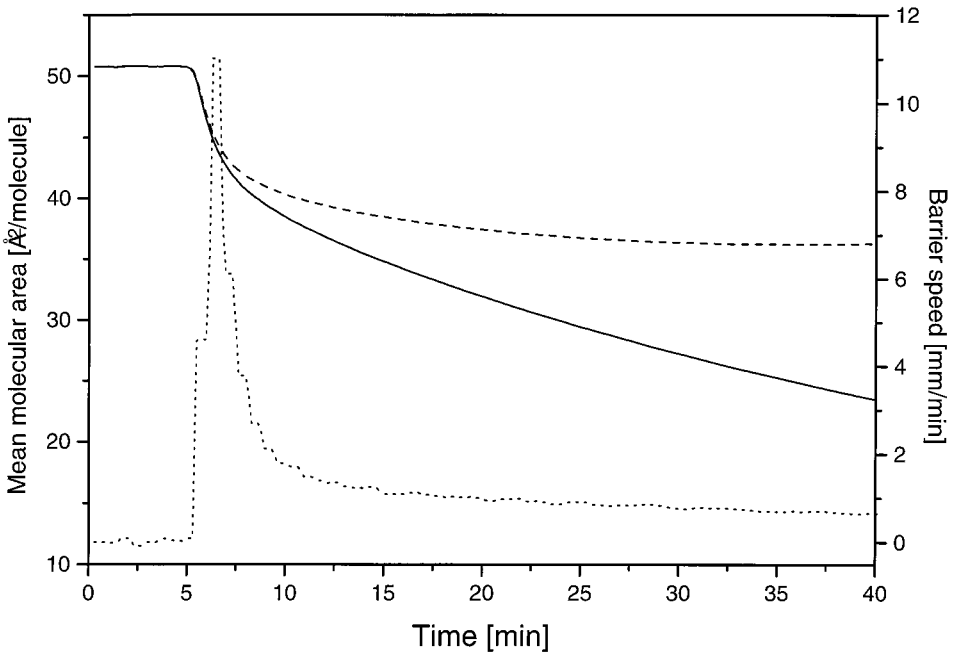

FIGURE 3 The barrier speed (- - -) and mean molecular area (——) versus time of a DLiPE monolayer during UV irradiation on a Tris/NaCl/UAc, pH 7.2 subphase. The UV light was switched on at time $t = 5$ min. Also included is the corrected mean molecular area (– – –).

indirect evidence that oxidation at fully compressed monolayers takes place only to a very minor extent, whereas cross-linking dominates. Based on these data, however, nothing can be concluded about the molecular weight of the end product. The monolayers UV-irradiated at low (<30 mN/m) pressures were not further studied because of the observed expansion.

The reaction kinetics of DLiPE was also followed by UV-vis spectroscopy. LB films of DLiPE were deposited on quartz/Tb stearate plates at a surface pressure of 30 mN/m, after which the UV-vis spectra of the LB films were measured after different irradiation times. The spectra obtained for a 12-layer sample deposited from a Tris/NaCl/UAc subphase are shown in Fig. 4. The inset shows the spectra obtained for a 10-layer sample deposited from a IEW/UAc subphase. Fig. 4 clearly shows how the absorbance band at 235 nm decreases and finally disappears with proceeding irradiation, which is an indication of a cross-linking process. The data also indicate that the reaction was fully completed after ~20 min of UV irradiation. We also irradiated the DLiPE monolayers before they were deposited on a quartz plate and measured the UV-vis spectra for the deposited films (data not shown). The results showed the same features as in Fig. 4, but the nonperfect deposition of the

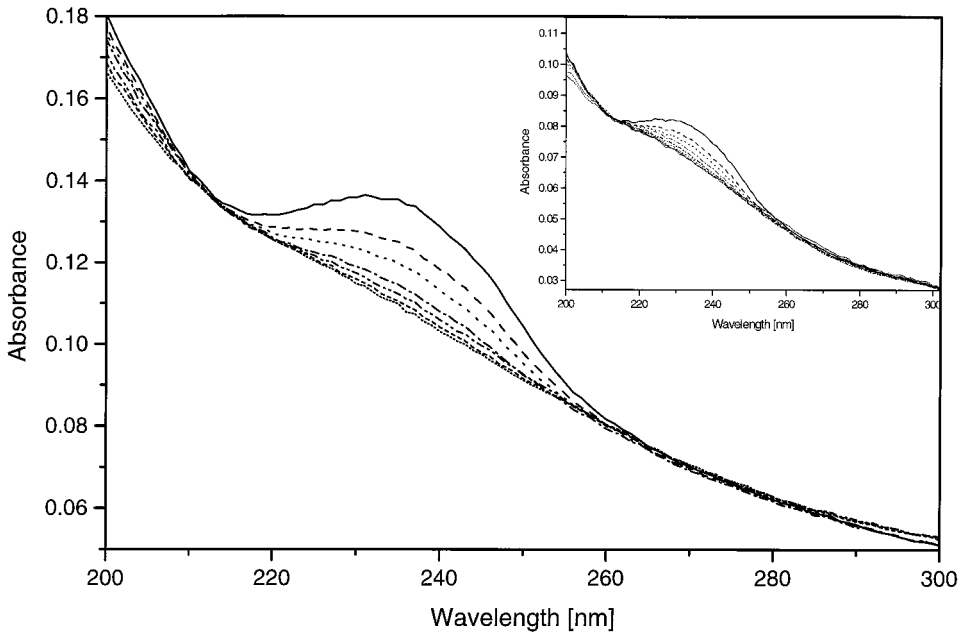

FIGURE 4 UV-vis spectra of a DLiPE LB film (12 layers) UV-irradiated for different times after deposition from a Tris/NaCl/UAc (pH 7.2) subphase at 30 mN/m. Monomer (——), 37 s UV-irradiated (— —), 75 s UV-irradiated (- - -), 2.5 min UV-irradiated (– · –), 5 min UV-irradiated (– · · –), 10 min UV-irradiated (– – –), and 20 min UV-irradiated (·····). The inset shows the same for a 10-layer sample deposited from a IEW/UAc (pH 4.7) subphase at 30 mN/m: monomer (——), 30 s UV-irradiated (— —), 1 min UV-irradiated (- - -), 2 min UV-irradiated (– · –), 4 min UV-irradiated (– ·· –), 8 min UV-irradiated (– – –), and 16 min UV-irradiated (·····).

irradiated monolayers inhibited the quantitative analysis of these results.

FTIR spectroscopy

The FTIR spectra of monomeric and UV-irradiated DLiPE films are shown in Fig. 5. The following characteristic peaks were found in the spectra (the wavenumbers refer to the peaks of the monomeric film) (Blume, 1996; Rabolt et al., 1983; Peltonen et al., 1994): the CH_3 stretching vibrational bands at 2953 cm^{-1} (asymmetrical) and 2870 cm^{-1} as a shoulder (symmetrical); the strong peaks due to CH_2 stretching vibrations at 2926 cm^{-1} (asymmetrical) and 2854 cm^{-1} (symmetrical); the important but quite weak peak due to the carbon-carbon double bond at 3013 cm^{-1}; the broad band at 3100–3400 cm^{-1}, referring to the hydroxy complex of the UAc-$(lipid)_2$ dimers and the hydroxy group of water; the ester carbonyl stretching band at 1740 cm^{-1}; the CH_2 bending and wagging bands at 1452 cm^{-1} and 1340 cm^{-1}; the CH_3 symmetrical bending band at 1380 cm^{-1}; the CO-O-C antisymmetrical and symmetrical stretching bands at 1180 and 1102 cm^{-1}; the phosphate ester stretching band at 1072 cm^{-1}; and the OH band at 920 cm^{-1} characteristic of the hydroxy-UAc complex. The absence of the 920 cm^{-1} band in the solution spectrum (not shown) indicates that this band arises from the hydroxy complexes associated with the UAc-$(lipid)_2$ dimers. The CH_2 progression band normally seen as a broad band at 1200–1350 cm^{-1} was weak for the monomeric film and practically absent for the irradiated film, indicating that the chain vibration becomes more restricted or that the crystallinity of the film decreases as a result of irradiation. The irradiation-induced changes could be identified as follows: the double-bond band at 3013 cm^{-1} disappeared, and the system became more disordered, as indicated by the decreased intensity and slight blueshift of the CH_2 and CH_3 vibrational and CH_3 bending bands. The irradiated film also seemed to adsorb slightly more water than the monomeric film, which was seen as an increased relative absorbance intensity of the 3100–3400 cm^{-1}, 920 cm^{-1}, and 1600–1700 cm^{-1} (characteristic band for water) bands. However, no new bands appeared as a result of irradiation, indicating that, e.g., the contribution arising from possible oxidation is ruled out. It also seems obvious that the deposition yield of the irradiated film is fair enough to allow the fabrication of a multilayer structure—this would not be possible for a monolayer being destroyed by UV light.

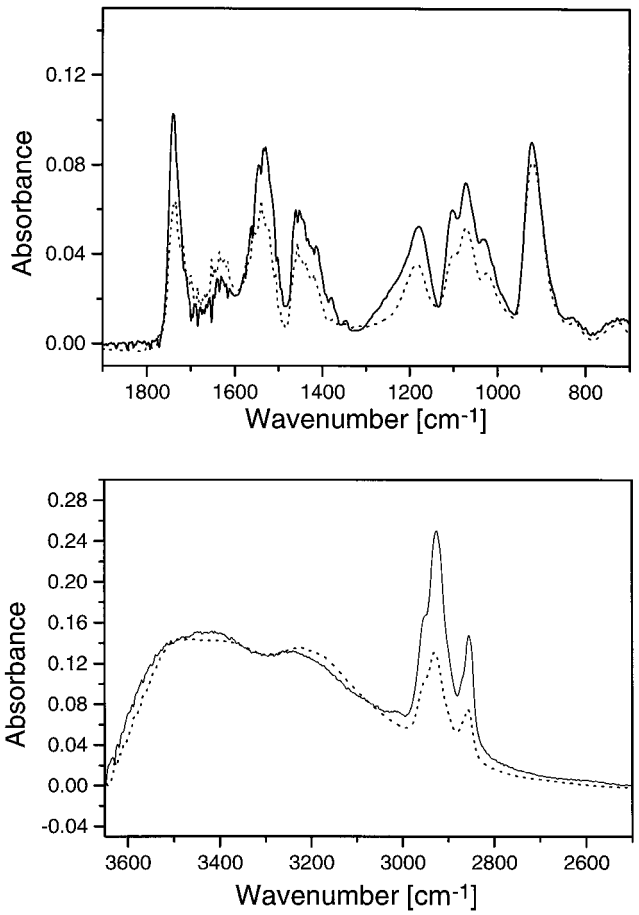

FIGURE 5 ATR-FTIR spectra of a DLiPE multilayer structure (eight layers) deposited horizontally from a IEW/UAc subphase at 30 mN/m before UV irradiation (——) and after 20 min of UV irradiation (– – –).

Kinetic models

The reaction kinetics of LA has been shown to follow a first-order kinetic model, and the assumption that DLiPE would follow the same model is justified by the fact that the two molecules have the same reactive sites. Therefore we proceeded with DLiPE as earlier with LA (Viitala et al., 1997). The decrease in the absorbance band at 235 nm with irradiation time (Fig. 4) was used to adapt a first-order model derived from the general first-order reaction kinetic equation described in the literature, using the equation

$$\ln [A(t)/A(0)] = -k \times t \quad (1)$$

where $A(t)$ is the absorbance at time t and $A(0)$ is the absorbance for a nonirradiated monolayer for the absorbance band centered at 235 nm. The absorbance value can be used directly because the concentration should be directly proportional to the absorbance. The result of this kind of adaptation to the UV-vis data is shown in Fig. 6. It can clearly be seen that the data points in Fig. 6 do not show a linear time dependence, which should be the case if the reaction were following first-order kinetics. A probable explanation for the deviation from linearity is that we have applied a model that mainly is applicable in three dimensions, whereas our system is a two-dimensional system to a reasonable approximation. This clearly shows that the monomer concentration is not constant in the vicinity of the reacting molecules after the LB film has been irradiated for a longer time, leading to deviations from linearity. Hence, in the model, one must also consider the time-dependent area variation in conjunction with the time-dependent change in

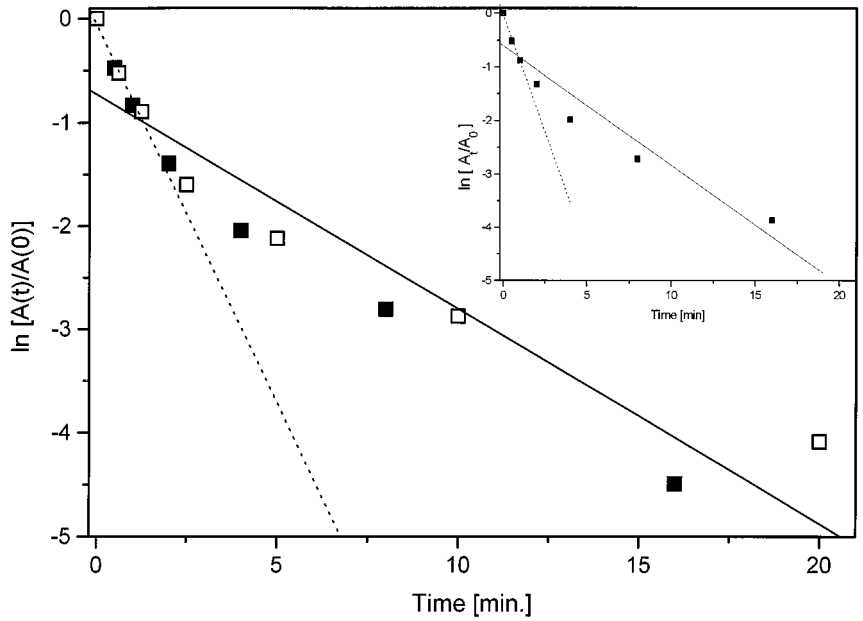

FIGURE 6 Adaptation of Eq. 1 to the data obtained from the LB UV-irradiation experiments (cf. Fig. 4). Six-layer (■) and 12-layer (□) samples were deposited at 30 mN/m from a Tris/NaCl/UAc (pH 7.2) subphase. The inset shows the same for a 10-layer sample deposited at 30 mN/m from an IEW/UAc (pH 4.7) subphase. ——, The linear regression line fitted to the data points. ·····, What is referred to in the text as the "initial slope."

the monomer concentration near the reaction centers. This concept was first introduced successfully by Rolandi et al. (1995). These two effects can be considered by the combination of the independently measured data obtained from UV-vis spectra (Fig. 4) and the UV-induced area reduction (Fig. 3, *dashed line*). Introducing both concepts in the first-order kinetics equation gives the following equation (Viitala et al., 1997):

$$\mathrm{d}[N(t)/N(0)]/\mathrm{d}t - \{[N(t)/N(0)]/A(t)\} \times \{\mathrm{d}A(t)/\mathrm{d}t\} = -k \times [N(t)/N(0)] \quad (2)$$

Plotting the left-hand side of Eq. 2 as a function of $N(t)/N(0)$ should give a straight line with the slope corresponding to $-k$. The adaptation of Eq. 2 to our data is shown in Fig. 7. The correlation coefficient of the linear regression line fitted to the data points is 0.996 for both cases, indicating a very good fit. The reaction kinetic constants obtained for monolayers on Tris/NaCl/UAc and IEW/UAc subphases were $130 \times 10^{-4}\ \mathrm{s}^{-1}$ and $156 \times 10^{-4}\ \mathrm{s}^{-1}$, respectively, which is slightly larger than the value obtained earlier for LA, $117 \times 10^{-4}\ \mathrm{s}^{-1}$. When only the initial slope (the first minute) of the data in Fig. 4 is considered, the reaction kinetic constants obtained are $130 \times 10^{-4}\ \mathrm{s}^{-1}$ and $146 \times 10^{-4}\ \mathrm{s}^{-1}$. Obviously the respective values obtained coincide with each other, thus justifying the conclusion that when a two-dimensional reaction has a large area reduction, one should use at least two different measuring techniques

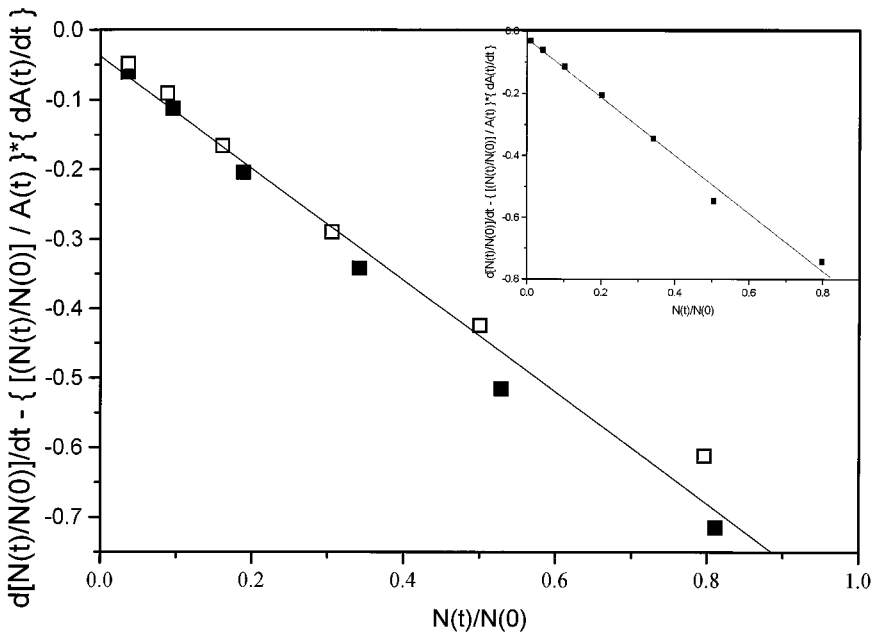

FIGURE 7 The left side of Eq. 2, plotted as a function of $N(t)/N(0)$. Six-layer (■) and 12-layer (□) samples were deposited at 30 mN/m from a Tris/NaCl/UAc (pH 7.2) subphase. The inset shows the same for a 10-layer sample deposited at 30 mN/m from an IEW/UAc (pH 4.7) subphase. The solid line is the linear regression line fitted to the data points.

that give complementary information about the time-dependent components.

AFM measurements

From the point of view of monolayer homogeneity, it was challenging to study the topographical features of the prepared multilayer structures, as a function of both subphase composition and UV irradiation time. The strong enhancing effect of the UAc ions on the monolayer homogeneity is demonstrated in Fig. 8. When depositing from a Tris/NaCl subphase, the striking feature was a transfer ratio of ~2 during the downstroke of the mica/Tb stearate substrate, indicating a bilayer transfer. During the upstroke, a negative transfer ratio (~−0.5) was observed. Therefore it seems obvious that the holes (monolayer-free areas) are the result of a partial desorption of the first monolayer that was deposited in the bilayer form. The bilayer structure is confirmed by the height difference between the film-free and film-covered areas, which was (4.7 ± 0.3) nm, as measured by the bearing analysis. This value is realistic when the nonlinearity of the unsaturated acyl chains is taken into account. A monolayer thickness of 2.5 nm for DLiPE measured by AFM has been reported (Hui et al., 1995), which further supports our result. The bilayer deposition during the downstroke refers to marked changes in the morphology of the floating monolayer on a Tris/NaCl subphase and is probably connected to the unequal cross section of the headgroup and hydrocarbon tails of DLiPE (Israelachvili et al., 1976).

The introduction of UAc in the subphase increased the homogeneity of the built-up LB films remarkably (Fig. 8 *b*). The equal transfer ratios of ~1.1 for the down- and upstrokes indicated a homogeneous transfer process. The surface of the deposited films still contains holes but is clearly continuous, as compared with the UAc-free film of Fig. 8 *a*. Holes corresponding to both monolayer and bilayer thicknesses exist to an equal extent on the surface, with respective depth values of (2.7 ± 0.2) nm and (5.0 ± 0.3) nm. The slightly increased bilayer thickness is believed to result from the increased condensation of the monolayer, reflecting the more vertically aligned lipid molecules as compared with the UAc-free film. This series of AFM images thus further explains the enhanced homogeneity and reactivity of the UAc-DLiPE monolayers.

The influence of the UV irradiation on the film topography is demonstrated in Fig. 9. As compared with the monomer film (Fig. 9 *a*), 0.5 min of irradiation already affects the topology of the film (Fig. 9 *b*). The holes have increased in lateral size but decreased in number. After 2.5 min of irradiation (Fig. 9 *c*) the changes are minor. However, very small new holes have appeared in the continuous film. After 20 min of irradiation, these small holes are already clearly visible on the film surface (Fig. 9 *d*). Fig. 9 demonstrates that the DLiPE film remains as a true planar film throughout the irradiation process, even if the holes interrupt the otherwise continuous surface. The birth of small new holes in the structure after 2.5 min of irradiation may be regarded as the start of gradual film degradation. The phenomenon is clearly amplified in Fig. 9 *d*, with additional marks of slight folding of the film at the hole edges. However, the magnitude of folding is far from that observed earlier for LA, for which a clear two-phase (folded/nonfolded) structure has been reported (Peltonen and Viitala, 1996, 1998). Against this background, comparing LA and DLiPE, the latter seems to be a more suitable cross-linking agent with a slightly larger reaction rate constant and better topographical homogeneity of the resulting film.

To gain more information about the structure of the floating monolayers both the monomeric and 5-min UV-irradiated UAc-DLiPE films were allowed to stabilize at the air-water interface for 2 h at constant surface pressure

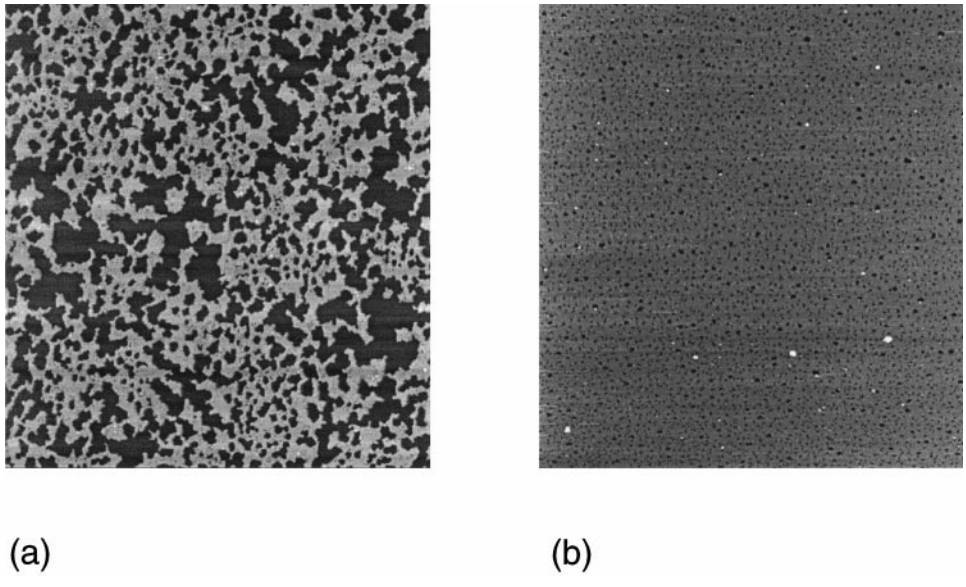

FIGURE 8 AFM tapping-mode images of bilayers of DLiPE on mica/Tb stearate deposited at 30 mN/m from two different subphases. (*a*) Tris/NaCl, pH 7.2. (*b*) Tris/NaCl/UAc, pH 7.2. The size and the dark-light height scale of the images are $10 \times 10\ \mu m^2$ and 8 nm, respectively.

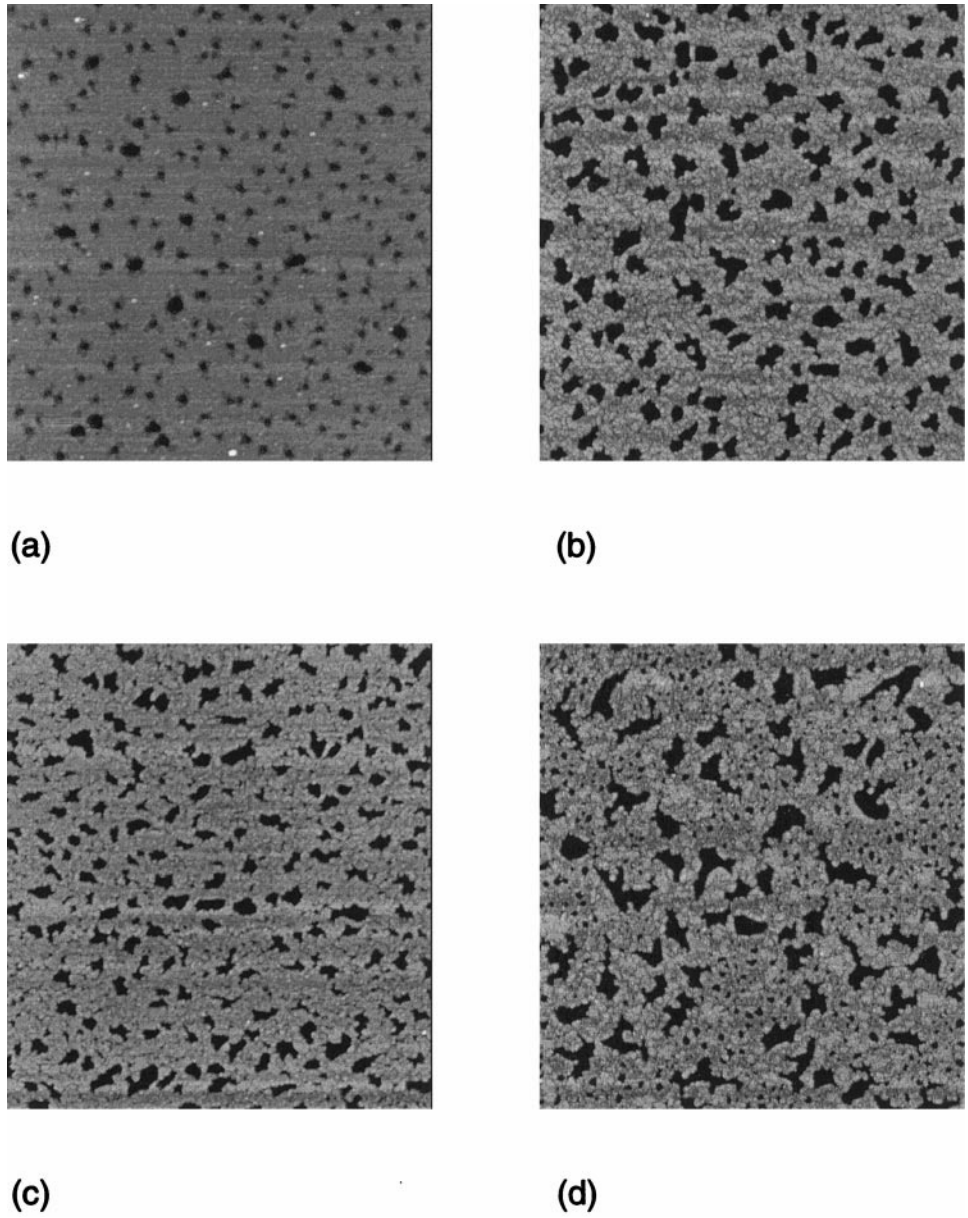

FIGURE 9 AFM tapping-mode images of bilayers of UV-irradiated DLiPE monolayers deposited on mica/Tb stearate at 30 mN/m from a Tris/NaCl/UAc, pH 7.2 subphase. The size and the dark-light height scale of the images are $2.5 \times 2.5\ \mu m^2$ and 8 nm, respectively. Monolayers were UV-irradiated for different times before deposition. (*a*) 0 min. (*b*) 0.5 min. (*c*) 2.5 min. (*d*) 20 min.

before a bilayer was deposited on a mica/Tb stearate substrate for AFM analysis. Fig. 10 shows the results. The monomeric sample (Fig. 10 *a*) has clearly transformed into a lipid particle form, whereas the UV-irradiated sample (Fig. 10 *b*) has remained as a planar true monolayer, even if containing the hole defects. This means that the UAc ions responsible for the enhanced condensation and homogeneity as compared with plain monomeric films (Fig. 9) are not enough to generate long-term stability, e.g., reorganization of the lipids clearly takes place. This kinetic process was clearly inhibited for the UV-irradiated films, indirect evidence that cross-linking as a stabilizing factor had taken place. The same kind of stabilizing effect could also be seen for multilayer samples of both monomeric and 5-min UV-irradiated UAc-DLiPE films (Fig. 10, *c* and *d*). It is clearly seen that the monomeric film is not stable enough to form a multilayer structure but ends up in a network structure of lipid particles with the characteristics of a wetting/dewetting process. The UV-irradiated monolayer, on the contrary, has remained as a monolayer, even though small particles also appear on the surface here. This indicates that the cross-linking does not fully inhibit but clearly slows down the monolayer instability, appearing as reorganization of lipid molecules.

CONCLUDING REMARKS

The use of UAc ions in the subphase made possible the condensation of a DLiPE Langmuir monolayer through a transition from a liquid-expanded to a solid-expanded state. This was evidenced by both the compression isotherms and AFM. The monolayer condensation was a prerequisite for a successful reaction of the monolayer. The evidence for the

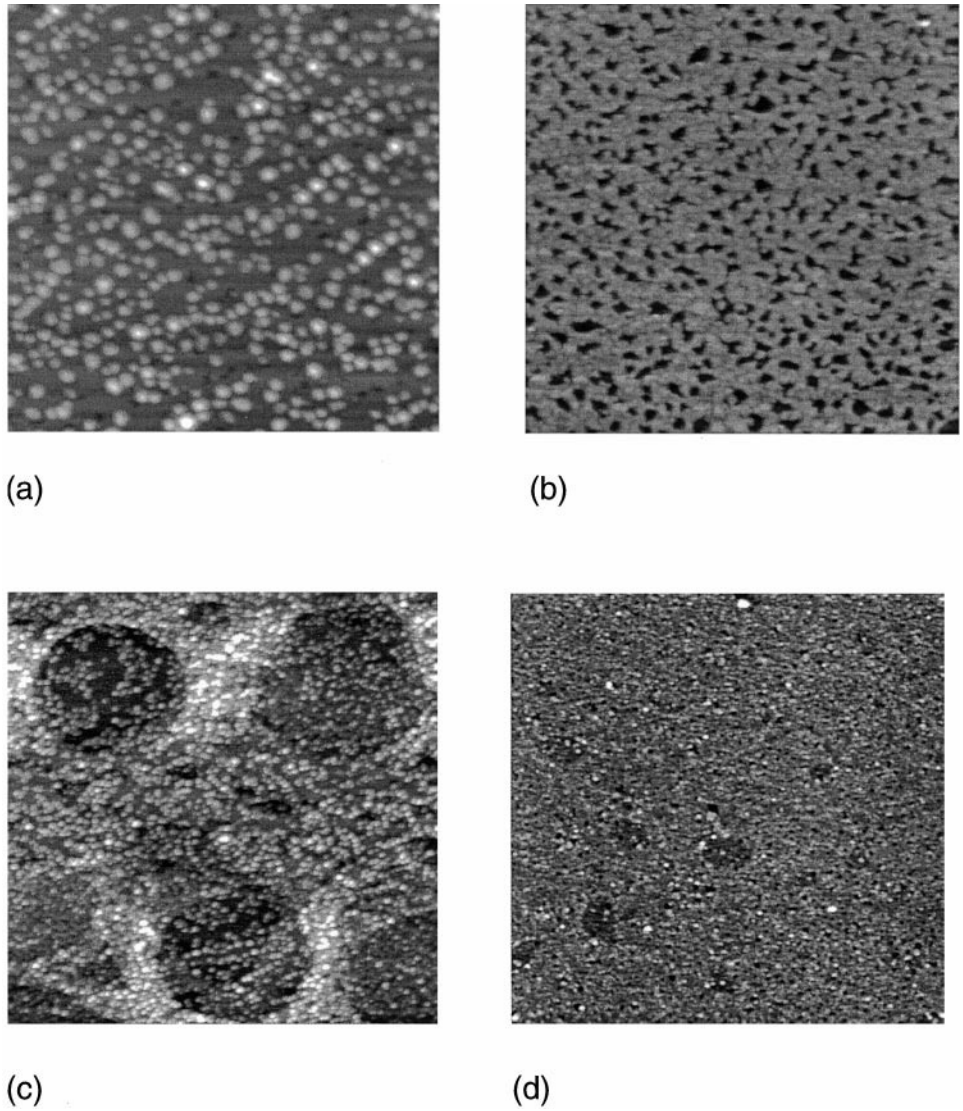

FIGURE 10 AFM tapping-mode images of a bilayer structure of (*a*) a monomeric and (*b*) a 5 min UV-irradiated Langmuir monolayer stabilized for 2 h before being deposited on a mica/Tb stearate substrate from a NaCl/Tris/UAc subphase. (*c,d*) The respective multilayer structures (10 layers) of (*c*) a monomeric and (*d*) a 5 min UV-irradiated Langmuir monolayer stabilized 15 min before being deposited. The size and the dark-light height scale of the *a* and *b* images are $2.5 \times 2.5\ \mu m^2$ and 30 nm and 10 nm, respectively, and those of the *c* and *d* images are $10 \times 10\ \mu m^2$ and 30 nm and 15 nm, respectively.

cross-linking reaction was obtained from the reaction kinetic measurements at the air-water interface, UV-vis and FTIR spectroscopy, and AFM. Furthermore, in contrast to solid-state reactions, the reaction in the solid-expanded state makes it possible for the molecules to reorient during the area contraction, which is typical for this system. The inhibited phase separation in the SE phase is expected to be an essential advantage in the future protein immobilization studies of mixed films of DLiPE and DLiPE-linker. The UV-induced reaction followed the same first-order reaction kinetic model that was used in the study of LA monolayer reactivity. The AFM images support the conclusion that the reaction is almost complete after just ~2 min of irradiation. Continued irradiation obviously leads to monolayer degradation.

The Academy of Finland (project no. 30591) is acknowledged for its financial support of this work. Petri Ihalainen's help on interpreting the FTIR data is acknowledged.

REFERENCES

Arslanov, V. V. 1992. Monolayers and Langmuir-Blodgett films of monomers and polymers: polyreactions, structural transformations, properties and applications. *Adv. Colloid Interface Sci.* 40:307–370.

Blume, A. 1996. Properties of lipid vesicles: FT-IR spectroscopy and fluorescence probe studies. *Curr. Opin. Colloid Interface Sci.* 1:64–77.

Bodalia, R. R., and R. S. Duran. 1993. Polymerization of 2-pentadecylaniline monolayers at fluid surfaces: kinetics, thermodynamics, and mechanism. *J. Am. Chem. Soc.* 115:11467–11474.

Brinkhuis, R. H. G., and A. J. Schouten. 1991. Monolayer behaviour of some stereoregular poly(methacrylates). *Langmuir.* 8:2247–2254.

Cemel, A., T. Fort, Jr., and J. B. Lando. 1972. Polymerization of vinyl stearate multilayers. *J. Polym. Sci.* 10:2061–2083.

Chapman, D., P. Byrne, and G. G. Shipley. 1966. The physical properties of phospholipids. I. Solid state and mesomorphic properties of some 2,3-diacyl-DL-phosphatidylethanolamines. *Proc. R. Soc. A.* 285: 115–142.

Dubault, A., C. Casagrande, and M. Veyssie. 1975. Two-dimensional polymerization processes in mono- and diacrylic esters. *J. Phys. Chem.* 79:2254–2259.

Fukuda, K., Y. Shibagaki, and H. Nakahara. 1988. Polymerizabilities of amphiphitic monomers with controlled arrangements in Langmuir–Blodgett films. *Thin Solid Films.* 160:43–52.

Gorwyn, D., and G. T. Barnes. 1990. Interactions of large ions with phospholipid monolayers. *Langmuir.* 6:222–230.

Hui, S. W., R. Viswanathan, J. A. Zasadzinski, and J. N. Israelachvili. 1995. The structure and stability of phospholipid bilayers by atomic force microscopy. *Biophys. J.* 68:171–178.

Israelachvili, J. N., D. J. Mitchell, and B. W. Ninham. 1976. Theory of self-assembly of hydrocarbon amphiphiles into micelles and bilayers. *J. Chem. Soc. Faraday Trans. II.* 72:1525–1568.

Laschewsky, A., H. Ringsdorf, and D. Schmidt. 1988. Polymerization of eicosenoic acid and octadecylfumarate in Langmuir-Blodgett multilayers. *Polymer.* 29:448–456.

Letts, S. A., T. Fort, Jr., and J. B. Lando. 1976. Polymerization of oriented monolayers of vinyl stearate. *J. Colloid Interface Sci.* 56:65–75.

Lindén, M., E. Györvary, J. Peltonen, and J. B. Rosenholm. 1995. UV-induced reactivity of linoleic acid monolayers. The influence of subphase conditions. *Colloids Surfaces A Physicochem. Eng. Aspects.* 102: 105–115.

Meller, P., R. Peters, and H. Ringsdorf. 1989. Microstructure and lateral diffusion in monolayers of polymerizable amphiphiles. *Colloid Polym. Sci.* 267:97–107.

Mino, N., H. Tamura, and K. Ogawa. 1991. Analysis of color transitions and changes on Langmuir-Blodgett films of a polydiacetylene derivative. *Langmuir.* 7:2336–2341.

Miyashita, T., and Y. Ito. 1995. Spreading behavior of polymerizable monolayers of acrylamides with double alkyl chains and polymerization of the LB films. *Thin Solid Films.* 260:217–221.

Ogawa, K. 1989. Study on polymerization mechanism of pentacosadiynoic acid Langmuir-Blodgett films using high energy beam irradiations. *J. Phys. Chem.* 93:5305–5310.

Peltonen, J. P. K., P. He, M. Lindén, and J. B. Rosenholm. 1994. Phase-controlled polymerization of linoleic acid monolayers. *J. Phys. Chem.* 98:12403–12409.

Peltonen, J. P. K., P. He, and J. B. Rosenholm. 1992. The polymerization of monolayers of some unsaturated fatty acids. *Thin Solid Films.* 210/211:372–374.

Peltonen, J. P. K., P. He, and J. B. Rosenholm. 1993. Influence of UV irradiation on unsaturated fatty acid monolayers and multilayer films: x-ray diffraction and atomic force microscopy study. *Langmuir.* 9:2363–2369.

Peltonen, J. P. K., and J. B. Rosenholm. 1989. The influence of light on the properties of fatty acid-poly(3-octylthiophene) Langmuir-Blodgett films. *Thin Solid Films.* 179:543–547.

Peltonen, J., and T. Viitala. 1996. Topographical studies of Langmuir-Blodgett films polymerized as a floating monolayer. *Polym. Preprints.* 37:604–605.

Peltonen, J., and T. Viitala. 1998. Atomic force microscopy of Langmuir-Blodgett films polymerized as a floating monolayer. *ACS Symp. Ser.* 694:231–249.

Peñacorada, F., J. Reiche, S. Katholy, L. Brehmer, and M. L. Rodríguez-Méndez. 1995. Monolayers and multilayers of uranyl arachidate. 1. Study of the interaction of dissolved uranyl ions with arachidic acid Langmuir monolayers. *Langmuir.* 11:4025–4030.

Rabolt, J. F., F. C. Burns, N. E. Schlotter, and J. D. Swalen. 1983. Anisotropic orientation in molecular monolayers by infrared spectroscopy. *J. Chem. Phys.* 78(2):946–952.

Raudino, A. 1994. Some theoretical considerations on diffusion-controlled one-chain polymerization in two-dimensional systems. *J. Polym. Sci. B Polym. Phys.* 32:2311–2320.

Ringsdorf, H., and H. Schupp. 1982. Polymerization of substituted butadienes at the gas-water interface. *In* Interfacial Synthesis, Vol. 3. C. E. Carraher and J. Preston, editors. Marcel Dekker, New York. 335–346.

Roberts, G. G. 1990. Langmuir-Blodgett Films. Plenum Press, New York.

Rolandi, R., S. Dante, A. Gussoni, S. Leporatti, L. Maga, and P. Tundo. 1995. Polymerized monomolecular films: microscopic structure, viscosity, and polymerization kinetics. *Langmuir.* 11:3119–3129.

Tamres, M., and J. Yarwood. 1973. *In* Spectroscopy and Structure of Molecular Complexes. J. Yarwood, editor. Plenum Press, London. 218.

Tancrede, P., L. Parent, P. Paquin, and R. M. LeBlanc. 1981. Interactions in mixed monolayers between dioleoyl-L-phosphatidylcholine and all-*trans* retinal. *J. Colloid Interface Sci.* 83:606–613.

Tieke, B., H.-J. Graf, G. Wegner, B. Naegele, H. Ringsdorf, A. Banerjie, D. Day, and J. B. Lando. 1977. Polymerization of mono- and multilayer forming diacetylenes. *Colloid Polym. Sci.* 255:521–531.

Tieke, B., G. Lieser, and G. Wegner. 1979. Polymerization of diacetylenes in multilayers. *J. Polym. Sci. Polym. Chem. Ed.* 17:1631–1644.

Tillmann, R. W., U. G. Hofmann, and H. E. Gaub. 1994. AFM investigation of the molecular structure of films from a polymerizable two-chain lipid. *Chem. Phys. Lipids.* 73:81–89.

Tocanne, J.-F., and J. Teissié. 1990. Ionization of phospholipids and phospholipid-supported interfacial lateral diffusion of protons in membrane model systems. *Biochim. Biophys. Acta*. 1031:111–142.

Toth, L. M., and G. M. Begun. 1981. Raman spectra of uranyl ion and its hydrolysis products in aqueous HNO_3. *J. Phys. Chem.* 85:547–549.

Turro, N. J. 1978. Modern Molecular Photochemistry. Benjamin/Cummings Publishing, Redwood City, CA. 135–148.

Viitala, T. J. S., J. Peltonen, M. Lindén, and J. B. Rosenholm. 1997. Spectroscopy, polymerization kinetics and topography of linoleic acid Langmuir and Langmuir-Blodgett films. *J. Chem. Soc. Faraday Trans.* 93:3185–3190.

Wang, L.-F., J.-F. Kuo, and C.-Y. Chen. 1995. Study on the properties of polyvinylacetate film at the air-water interface. *Colloid Polym. Sci.* 273:426–430.

Warta, R., and H. Sixl. 1988. Optical absorption and fluorescence spectroscopy of stable diacetylene oligomer molecules. *J. Chem. Phys.* 88:95–99.

Wayne, R. P. 1988. Principles and Applications of Photochemistry. Oxford University Press, New York.

Wegner, G. 1969. Polymerisation von derivaten des 2,4-hexadiin-1,6-diols im kristallin zustand. *Z. Naturforsch.* 24b:824–832.

Williams, D.H., and I. Fleming. 1966. Spectroscopic Methods in Organic Chemistry. McGraw-Hill, London. 12.

Yang Xiao-Min, Guang-Wei Min, Ning Gu, Zu-Hong Lu, and Yu Wei. 1994. Investigation of molecular chains structure of polyimide Langmuir-Blodgett films by atomic force microscopy. *J. Vac. Sci. Technol.* B12:1981–1983.